HHS Public Access

Author manuscript

J Magn Reson Imaging. Author manuscript; available in PMC 2020 January 24.

Published in final edited form as:

J Magn Reson Imaging. 2019 April ; 49(4): 917–926. doi:10.1002/jmri.26542.

Renal and Adrenal Masses Containing Fat at MRI: Proposed Nomenclature by the Society of Abdominal Radiology Disease-Focused Panel on Renal Cell Carcinoma

Nicola Schieda, MD[1,*], **Matthew S. Davenport, MD, PhD**[2], **Ivan Pedrosa, MD**[3], **Atul Shinagare, MD**[4], **Hersch Chandarana, MD, PhD**[5], **Nicole Curci, MD**[2], **Ankur Doshi, MD**[5], **Gary Israel, MD**[6], **Erick Remer, MD**[7], **Jane Wang, MD**[8], **Stuart G. Silverman, MD**[4]

[1]Department of Medical Imaging, From the University of Ottawa, Ottawa Hospital, Ottawa, Ontario, Canada;

[2]Department of Radiology, Michigan University, Ann Arbor, Michigan, USA;

[3]Department of Radiology, UT Southwestern, Dallas, Texas, USA;

[4]Department of Radiology, Brigham and Women's Hospital, Boston, Massachusetts, USA;

[5]Department of Radiology, NYU School of Medicine, New York, New York, USA;

[6]Department of Radiology, Yale University, New Haven, Connecticut, USA;

[7]Department Radiology and Diagnostic Imaging, Cleveland Clinic, Cleveland, Ohio, USA;

[8]Department of Radiology, UCSF, San Francisco, California, USA

Abstract

This article proposes a consensus nomenclature for fat-containing renal and adrenal masses at MRI to reduce variability, improve understanding, and enhance communication when describing imaging findings. The MRI appearance of "macroscopic fat" occurs due to a sufficient number of aggregated adipocytes and results in one or more of: 1) intratumoral signal intensity (SI) loss using fat-suppression techniques, or 2) chemical shift artifact of the second kind causing linear or curvilinear India-ink (etching) artifact within or at the periphery of a mass at macroscopic fat–water interfaces. "Macroscopic fat" is most commonly observed in adrenal myelolipoma and renal angiomyolipoma (AML) and only rarely encountered in other adrenal cortical tumors and renal cell carcinomas (RCC). Nonlinear noncurvilinear signal intensity loss on opposed-phase (OP) compared with in-phase (IP) chemical shift MRI (CSI) may be referred to as "microscopic fat" and is due to: a) an insufficient amount of adipocytes, or b) the presence of fat within tumor cells. Determining whether the signal intensity loss observed on CSI is due to insufficient adipocytes or fat within tumor cells cannot be accomplished using CSI alone; however, it can be inferred when other imaging features strongly suggest a particular diagnosis. Fat-poor AML are homogeneously hypointense on T_2-weighted (T_2W) imaging and avidly enhancing; signal intensity loss at OP CSI is uncommon, but when present is usually focal and is caused by an insufficient number of

[*]Address reprint requests to: N.S., University of Ottawa, Ottawa Hospital, Department of Medical Imaging, 1053 Carling Ave., Ottawa, ON, Canada K1Y 4E9. nschieda@toh.on.ca.

Additional supporting information may be found in the online version of this article.

adipocytes within adjacent voxels. Conversely, clear-cell RCC are heterogeneously hyperintense on T_2W imaging and avidly enhancing, with the signal intensity loss observed on OP CSI being typically diffuse and due to fat within tumor cells. Adrenal adenomas, adrenal cortical carcinoma, and adrenal metastases from fat-containing primary malignancies also show signal intensity loss on OP CSI due to fat within tumor cells and not from intratumoral adipocytes.

DETECTION OF FAT in adrenal and renal masses at magnetic resonance imaging (MRI) can be a critical finding to help formulate an imaging diagnosis.[1–6] The presence of macroscopic fat almost always indicates a benign diagnosis; however, adrenal cortical carcinomas (ACC) and renal cell carcinomas (RCC) often contain small quantities of fat within the cytoplasm of tumor cells, which may be detectable using chemical shift MRI (CSI), a feature that has been described as an imaging pitfall in the MR evaluation of adrenal and renal masses (Fig. 1).[1,7,8] Adding to this potential interpretive pitfall is the wide array of radiological terms used to describe the presence of fat in adrenal and renal masses at MRI. The terms “bulk fat,” “macroscopic fat or lipid,” “microscopic fat or lipid,” “intravoxel fat or lipid,” “intracellular fat or lipid,” and “intracytoplasmic fat or lipid” all have been used in benign and malignant adrenal and renal masses.[3,9,10]

A typical example of the varying and confusing terminology used to describe fat content at MRI occurs in the imaging description of smooth-muscle-predominant renal angiomyolipomas (AML), which have insufficient amounts of adipocytes (ie, fat cells) to cause detectable signal intensity loss when fat-suppression (FS) techniques are applied.[3,11] These tumors have been described on imaging as being “fat poor,” “lipid poor,” “fat invisible,” or “showing minimal or no visible or detectable fat or lipid.”[9] In this Commentary, a simplified nomenclature for the description of fat in adrenal and renal masses detected at MRI is proposed using a histological reference by the Society of Abdominal Radiology Disease Focused Panel on Renal Cell Carcinoma. The goals are to improve understanding by radiologists, trainees, and referring providers; improve communication; standardize terms for use in research; and reduce diagnostic errors.

PROPOSED NOMENCLATURE FOR DESCRIPTION OF FAT AT MRI IN ADRENAL AND RENAL MASSES WITH HISTOLOGICAL CORRELATION

An algorithm for the basis of the proposed nomenclature for adrenal and renal masses is provided in Figs. 2 and 3. Generally, we prefer the term fat over lipid because lipid is a broader term that encompasses the entire class of organic molecules that are insoluble in water, including those lipids that are not components of human tissues, while fat is the specific subclass of lipid that pertains to the histological findings observed in adrenal and renal masses.[12]

Macroscopic Fat

The imaging term “macroscopic fat” should be applied when a tumor shows one or more of the following: 1) intratumoral signal intensity loss before and after application of FS, or 2) linear or curvilinear chemical shift artifact of the second kind causing India-ink (etching) artifact within or at the periphery of the mass at macroscopic fat–water interfaces while the

central area remains hyperintense (ie, following the signal intensity of subcutaneous and intraabdominal fat). In the case of signal intensity loss due to FS techniques, the signal from protons within fat molecules has been nulled and is achieved using either chemical (spectral) FS, inversion recovery (IR), or a combination of chemical FS and IR (spectral + IR). More recently, water excitation techniques and 2- or 3-point fat and water separation algorithms derived from Dixon techniques also can be used to demonstrate the presence of macroscopic fat.[13] It is important to emphasize that nonspectral fat suppression techniques, such as IR, will lead to a nonselective decrease in signal intensity of other tissues with relatively short T_1 relaxation times (eg, proteinaceous and hemorrhagic contents) and thus, distinction between these tissues and fat cannot be achieved using IR.[14] Chemical shift artifact of the second kind, which occurs on T_1-weighted (T_1W) dual-echo chemical shift gradient recalled echo (GRE), is due to the cancellation of the signal of coexistent fat and water protons within the same imaging voxel, as their phase shift opposes one another due to differing precessional frequencies at the intentionally selected echo time (TE) during the OP acquisition.[15,16] Chemical shift artifact of the second kind also may be used as an imaging feature to diagnose the presence of macroscopic fat, and manifests as linear or curvilinear signal loss occurring either within or at the periphery of the mass at macroscopic fat–water interfaces.[17] Notably, the central area of macroscopic fat surrounded by the chemical shift artifact should remain hyperintense on both IP and OP images, matching the signal of macroscopic fat elsewhere in the abdomen.

The histological basis for identification of macroscopic fat within a mass at MRI relates to the presence of a sufficient amount of adipocytes (ie, fat cells)[11]; however, the biological cause for why a mass contains adipocytes depends on the nature of the mass. This imaging finding can be seen in classic renal angiomyolipomas and adrenal myelolipomas (Figs. 4,5).[2,6,10,11] To our knowledge, the sensitivity of detecting macroscopic fat has not been formally compared between FS techniques and chemical shift MRI; however, when areas of intratumoral fat are small (<1 cm), chemical shift MRI may outperform unenhanced computed tomography (CT) for the detection of macroscopic fat in small AMLs.[18] The use of 3D Dixon-based techniques allows for higher spatial resolution than conventional 2D CSI in a given breath-hold and this results in improved detection of fat in small (<1 cm) AMLs.[19]

Microscopic Fat

The imaging term “microscopic fat” should be applied when a tumor shows nonlinear noncurvilinear focal or diffuse signal intensity loss comparing opposed-phase (OP) to in-phase (IP) dual-echo T_1W GRE images. We prefer the term “microscopic fat” to “intracellular fat or lipid” or “intracytoplasmic fat or lipid” because all forms of fat within the body are by definition located within the cytoplasm of cells, including fat located within the cytoplasm of adipocytes and fat located within the cytoplasm of tumor cells. Similarly, the term “intravoxel fat” (which has also been used previously), although technically correct, is suboptimal because all forms of fat in the body are located to varying degrees within a given imaging voxel. The term microscopic fat is intended to convey an imaging observation that occurs due to the presence of fat on CSI that is not detectable using the means described in the section on macroscopic fat.

Signal intensity loss on OP compared with IP images in renal and adrenal masses due to microscopic fat can occur in two ways: 1) an insufficient amount of adipocytes, or 2) the presence of fat within tumor cells. In both cases, signal intensity loss on OP imaging is caused by chemical shift artifact of the second kind occurring because there are water and fat protons sharing the same imaging voxel. If adipocytes become sufficient in number (ie, only fat protons are identified within imaging voxels), the imaging finding of macroscopic fat will result. In the case of fat-poor AML, microscopic fat observed on CSI is due to an insufficient number of adipocytes (Fig. 5).[11] Conversely, in adrenal cortical tumors and RCC (predominantly clear cell subtype), signal intensity loss on OP compared with IP images occurs due to the presence of fat within the cytoplasm of tumor cells and is not related to the presence of adipocytes (Figs. 1, 6).[20–22]

It is not possible to differentiate the histological causes of microscopic fat using CSI alone. However, if the cause is suspected based on other imaging features (eg, based on signal intensity profile on other pulse sequences indicating a specific diagnosis) or is known (eg, research and educational settings, known histology), then the imaging finding of microscopic fat should be described as either being related to insufficient adipocytes or fat within tumor cells. For example, the imaging finding of microscopic fat in adrenal adenoma or RCC should not be attributed to the presence of an insufficient number of adipocytes because adipocytes are only rarely observed in these tumors.[23–29]

DESCRIPTION OF ADRENAL AND RENAL MASSES BY THE PRESENCE AND TYPE OF FAT

Masses With Macroscopic Fat

ADRENAL MASSES.—The presence of macroscopic fat within an adrenal mass at imaging and the presence of adipocytes at histopathology generally indicates myelolipoma (Fig. 4).[2,6] At imaging, nearly all myelolipomas have macroscopic fat content; when ≥50% macroscopic fat content is present, myelolipoma can be diagnosed with confidence.[30] Macroscopic fat has been described at imaging in other adrenal cortical tumors, including adenomas with myelolipomatous degeneration (uncommon), ACC (rare), and pheochromocytoma (very rare)[31,32]; however, in these reported cases the fat content represents a small amount of the overall volume of the tumor.[7,28,29,33,34] The proposed biological mechanism for why adrenal masses besides myelolipoma may contain adipocytes is unclear but has been attributed to tumoral degeneration or de-differentiation.[7,34]

RENAL MASSES.—Macroscopic fat within a renal mass at imaging is virtually diagnostic of “classic” angiomyolipoma, which is composed of varying amounts of smooth muscle, immature vessels, and adipocytes.[35] Rarely, macroscopic fat may be observed within RCC often attributed to osseous metaplasia[27]; in such cases, in our experience, the macroscopic fat content is small, generally <10% of the total volume of the mass. Typically, when macroscopic fat is encountered in RCC, it is almost always accompanied by calcifications.[24–27] Engulfed perirenal, retroperitoneal, or renal hilar fat related to a large RCC may result in the appearance of macroscopic fat within the tumor, but in these cases the diagnosis can be achieved by noting the invasive morphology of the mass. The presence of calcifications or

rapid growth can be potential indicators of malignancy; however, MRI is generally insensitive to calcification. Additionally, there are case reports of macroscopic fat-containing RCC without calcification, and macroscopic fat-containing AMLs with calcification.[24–26,36–38] Therefore, the prospective diagnosis of RCC with macroscopic fat may be challenging. It is important to emphasize that the presence of macroscopic fat within a renal mass, regardless of the ratio of macroscopic fat to solid elements within the mass, is almost always diagnostic of renal AML except in rare instances.

Masses With Microscopic Fat

ADRENAL MASSES WITH MICROSCOPIC FAT DUE TO INSUFFICIENT ADIPOCYTES.—

The presence of microscopic fat resulting from an insufficient number of adipocytes is rare in adrenal masses. Adipocytes within adrenal masses (even rare masses) generally result in macroscopic fat at MRI (myelolipoma, myelolipomatous degeneration of adrenal cortical neoplasms [uncommon], ACC [rare]).[2,7,28,29,34,39] In myelolipomas with tiny (<1 cm) foci of fat, the fat foci may be so small that they may appear as microscopic fat.[40]

RENAL MASSES WITH MICROSCOPIC FAT DUE TO INSUFFICIENT ADIPOCYTES.—

Among renal masses with microscopic fat, in only fat-poor AML is this imaging finding due to the presence of insufficient adipocytes.[11] In this instance, the adipocytes within the tumor are too few or not sufficiently clustered to be detected as macroscopic fat.

Fat-poor AML can be differentiated from other renal masses through a combination of characteristic features at both CT and MRI with a high degree of accuracy.[9,41–46] Fat-poor AML are typically small (<4 cm) incidentally discovered masses that occur most commonly in female patients.[9] These tumors do not tend to hemorrhage,[43,47] are usually homogeneously hyperdense at unenhanced CT,[48] and virtually always low signal intensity on T_2-weighted (T_2W) MRI and an apparent diffusion coefficient (ADC) map.[41,42,46,49] Unlike papillary RCC, which also may be hyperdense at unenhanced CT and low signal intensity on T_2W and ADC, fat-poor AML are typically avidly enhancing (whereas papillary tumors show low-level progressive enhancement).[41,42,45,46,50,51]

Although microscopic fat initially was thought to be a characteristic finding of fat-poor AML,[52] it also is commonly present in RCC (usually clear cell, discussed below),[20] and recent studies demonstrate that a majority of fat-poor AML do not demonstrate any signal loss on OP CSI.[11,53,54] Jhaveri et al. found that microscopic fat is more commonly focal in fat-poor AML and more commonly diffuse in RCC.[53] A meta-analysis found that fat-poor AML show quantitatively more signal loss on OP MRI compared with all RCCs, but that the degree of signal loss was not significantly different compared with clear-cell RCC.[55]

We prefer the term fat-poor AML be used to describe an AML that has an insufficient number of adipocytes to result in macroscopic fat on imaging. Various other terms, imaging and histological definitions, and classifications for fat-poor AML have been proposed; however, their clinical usefulness is limited with the exception that those fat-poor AML that

show microscopic fat are more likely to be isoatte-nuating (rather than hyperattenuating) at unenhanced CT.[3,11]

ADRENAL MASSES WITH MICROSCOPIC FAT DUE TO FAT CONTAINED IN TUMOR CELLS.—Adrenal cortical adenomas characteristically contain intracytoplasmic fat within tumor cells. This fat is the necessary precursor for the bio-chemical formulation of adrenal cortical steroid hormones. The fat occurring in the cytoplasm of tumor cells is interspersed with water protons also located within the cell and this results in the imaging finding of microscopic fat. Detection of microscopic fat within an adrenal mass is typical for adenoma. Macroscopic fat in adrenal adenomas only occurs in the uncommon setting of myelolipomatous degeneration.[7]

At MRI, microscopic fat can be quantitatively or qualitatively assessed.[10,16] Microscopic fat in adenomas is usually but not always homogeneous. It has been previously reported that heterogeneous microscopic fat in adrenal nodules also is generally benign[56]; however, caution must be used in patients with an oncologic history to exclude the rare possibility of a collision tumor (ie, microscopic fat-containing adenoma and adjacent metastasis)[57] or the more common occurrence of a microscopic fat-containing metastasis (eg, clear-cell RCC, hepatocellular carcinoma [HCC]). Approximately 30% of adenomas will not have sufficient fat within their cytoplasm to result in an attenuation value less than 10 Hounsfield Units (HU), which is the optimal threshold to differentiate adenomas from metastases at unenhanced CT.[2,7] These adenomas have historically been referred to as “lipid poor” adenomas.[10,16] A proportion of “lipid poor” adenomas that measure between 10 and 30 HU can be shown to demonstrate microscopic fat using chemical shift MRI; however, MRI is generally not useful to characterize adrenal nodules that measure above 30 HU at unenhanced CT.[58] Such adenomas cannot be reliably distinguished from metastasis, and further imaging workup (eg, washout criteria at CT for nonhypervascular malignancies) may be required in patients with a known malignancy. We acknowledge that the terms “lipid rich” and “lipid poor” adenomas are unlikely to change based on the recommendation of this article, given that these terms are so widely used in the imaging literature; however, with respect to our proposed nomenclature and content of adrenal cortical cells, the terms “fat rich” and “fat poor” would likely be more precise.

ACCs usually can be readily differentiated from adenomas based on their large size (>4 cm), heterogeneous appearance, invasive features, and presence of metastatic disease.[2,59] ACC may contain microscopic fat due to fat within tumor cells since they are derived from the adrenal cortex; however, there also are reports of ACC containing small quantities of macroscopic fat.[28,29,39] A single case report[60] described macroscopic fat within pheochromocytoma at CT. No studies to our knowledge have described microscopic or macroscopic fat within pheochromocytoma at MRI.[61,62]

Metastases from microscopic and macroscopic fat-containing primary tumors (eg, clear-cell RCC, HCC, lipo-sarcoma) have been described as an imaging pitfall on CSI due to the presence of fat within tumor cells simulating an adenoma.[2,7,8] Knowledge of the primary malignancy is crucial in these instances as other traditional imaging tests such as washout-CT also may be falsely reassuring due to hypervascularity of the same malignancies (eg,

clear-cell RCC, HCC).[63] It has been shown that metastases tend to be more heterogeneously hyperintense on T_2W imaging compared with adenomas, and this characteristic may help distinguish between the two entities in relevant cases.[64,65]

RENAL MASSES WITH MICROSCOPIC FAT DUE TO FAT CONTAINED IN TUMOR CELLS.—A histologic hallmark of clear-cell RCC is the presence of glycogen and fat in the cytoplasm of tumor cells. Intracytoplasmic fat is stored in "lipid" droplets, which are composed of a neutral fat core (triglycer-ides, cholesterol-esters) surrounded by a phospholipid mono-layer and surface proteins.[66] Outwater et al. first described microscopic fat in clear-cell RCC.[20] This is now a popularly presented imaging pitfall encountered on renal mass MRI because inexperienced radiologists may misinterpret it as diagnostic of AML (Fig. 1). Studies investigating the algorithmic diagnosis of small renal masses with MRI have noted that the presence of a microscopic fat may distinguish clear-cell RCCs from oncocytic neoplasms (eg, chromophobe RCC and onco-cytoma), each of which is characteristically hyperintense on T_2W imaging.[41,42,44] Clear-cell RCC also have been shown to be more avidly enhancing compared with oncocytic neoplasms.[44,67] A minority of papillary tumors also may show microscopic fat, which has been speculated to be due to clear cell heterogeneity[68]; such tumors may be distinguished from fat-poor AML by their high signal intensity on T_2w imaging (compared with typical papillary RCCs).[69] Because fat accumulation in clear-cell RCC is a pathophysiologic process of the tumor cells, microscopic fat is identified on OP images within the viable portions of the tumor (ie, enhancing components); areas of necrosis and scar typically lack this finding.

One should not mistakenly attribute microscopic fat on CSI in clear-cell RCC to be due to the presence of glycogen, since glycogen does not cause signal intensity drop on OP CSI using available chemical shift MRI pulse sequences on 1.5 T or 3 T clinical scanners. A detailed description of the CSI physics pertaining to water and fat or glycogen protons is provided in the Appendix.

The detection of fat in tissues using chemical shift MRI was initially described by Dixon.[70] Several confounders need to be addressed for the accurate measurement of fat fraction (FF) with this technique, including: T_1 bias, T_2* decay, spectral complexity of fat, noise bias, and eddy currents.[71] In recent years, Reeder et al. proposed a Dixon-based technique for quantification of FF using multiecho 3D GRE acquisitions and multipeak fat modeling.[72–74] These techniques correct for the above-mentioned confounders, and are now available in most clinical MRI scanners, and allow for quantification of FF in the entire abdomen during in a single breath-hold.[75] Multipeak fat modeling takes into account the multiple spectral peaks of fat to allow for more accurate measures of FF.[71] These techniques have been evaluated for the measurement of intratumoral fat in ccRCC.[76] ccRCCs show heterogeneous accumulation of fat independent of their grade, although it has been shown that more aggressive tumors (International Society of Urological Pathology [ISUP] nuclear grade 4) tumors exhibit a statistically significant decrease in FF compared with ISUP grade 3 tumors. FF cor-relates positively with triglyceride (TG) levels, negatively with free fatty acids (FFA) and phospholipids in general, and negatively with phosphoethanolamine specifically.[76]

CONCLUSION

In conclusion, a simplified nomenclature for the description of fat at MRI in adrenal and renal masses is proposed to clarify potentially confusing terminologies. Macroscopic fat is one or more of the following: 1) intratumoral signal loss using fat-suppression techniques, or 2) chemical shift artifact of the second kind causing linear or curvilinear India-ink (etching) artifact within or at the periphery of the mass at macroscopic fat–water interfaces. Macroscopic fat is virtually diagnostic of adrenal myelolipoma (in adrenal masses) and AML (in renal masses), with uncommon and rare exceptions. Microscopic fat is intratumoral nonlinear noncurvilinear signal intensity loss at OP CSI and may occur due to: a) an insufficient number of adipocytes in adjacent voxels, or b) the presence of fat within tumor cells. It is not possible to differentiate these conditions using CSI alone, but the cause can be inferred when other imaging features suggest a particular diagnosis or when the diagnosis is known. In fat-poor AML, signal intensity loss on OP CSI is uncommon, but when present is usually focal and caused by disaggregated adipocytes. In clear-cell RCC and adrenocortical neoplasms, signal intensity loss on OP CSI is due to fat within tumor cells.

APPENDIX

The difference in the water and glycogen peaks in ex vivo spectroscopic analysis of liver specimens is approximately 1 (range 0.5–1.5) ppm[77] compared with the difference in fat and water peaks of 3.5 ppm.[16] The frequency shift (Δf) between protons within two differing substances is calculated $\delta \times (\gamma \times Bo)$ where; δ = the chemical shift between two substances, γ = gyromagnetic ratio of protons (which is 42.5 Hz) and Bo = external magnetic field strength.[16] Therefore, the frequency shift for fat and water protons is 3.5 ppm × 42.5 Hz × 1.5 T or 3 T, which equals 226 Hz at 1.5 T and 446 Hz at 3 T.[16] A frequency shift of 226 Hz at 1.5 T and 446 Hz at 3 T equates to water and fat protons being in phase every 1/225 Hz or 4.4 msec at 1.5 T and every 1/445 Hz or 2.2 msec at 3 T. Conversely, for water and glycogen the frequency shift is 1 ppm × 42.5 Hz × 1.5 T or 3 T, which equals 63.8 Hz at 1.5 T and 127.5 Hz at 3 T. These frequency shifts equate to water and glycogen protons being in phase every 1/63.8 Hz or 15.7 msec at 1.5 T and every 1/127.5 Hz or 7.8 msec at 3 T. Therefore, since the first opposed phase echo between water and glycogen occurs at roughly 7.9 msec at 1.5 T and 3.9 msec at 3 T it would not be expected that glycogen content could substantially contribute to any signal drop on opposed phase images obtained at 2.2 msec or 1.1 msec (optimized to detect maximal signal cancellation from fat and water protons) at 1.5 T and 3 T, respectively.

REFERENCES

1. Ramamurthy NK, Moosavi B, McInnes MD, Flood TA, Schieda N. Multiparametric MRI of solid renal masses: Pearls and pitfalls. Clin Radiol 2015;70:304–316. [PubMed: 25472466]
2. Schieda N, Siegelman ES. Update on CT and MRI of adrenal nodules. AJR Am J Roentgenol 2017;208:1206–1217. [PubMed: 28225653]
3. Jinzaki M, Silverman SG, Akita H, Nagashima Y, Mikami S, Oya M. Renal angiomyolipoma: A radiological classification and update on recent developments in diagnosis and management. Abdom Imaging 2014;39: 588–604. [PubMed: 24504542]
4. Bosniak MA. Angiomyolipoma (hamartoma) of the kidney: A preoperative diagnosis is possible in virtually every case. Urol Radiol 1981;3:135–142. [PubMed: 7340024]

5. Israel GM, Bosniak MA. How I do it: Evaluating renal masses. Radiology 2005;236:441–450. [PubMed: 16040900]
6. Elsayes KM, Mukundan G, Narra VR, et al. Adrenal masses: MR imaging features with pathologic correlation. Radiographics 2004;24(Suppl 1): S73–86. [PubMed: 15486251]
7. Schieda N, Al Dandan O, Kielar AZ, Flood TA, McInnes MD, Siegelman ES. Pitfalls of adrenal imaging with chemical shift MRI. Clin Radiol 2014;69:1186–1197. [PubMed: 25062926]
8. Taner AT, Schieda N, Siegelman ES. Pitfalls in adrenal imaging. Semin Roentgenol 2015;50:260–272. [PubMed: 26542427]
9. Lim RS, Flood TA, McInnes MD, Lavallee LT, Schieda N. Renal angiomyolipoma without visible fat: Can we make the diagnosis using CT and MRI? Eur Radiol 2018;28:542–553. [PubMed: 28779401]
10. Siegelman ES. Adrenal MRI: Techniques and clinical applications. J Magn Reson Imaging 2012;36:272–285. [PubMed: 22807221]
11. Hakim SW, Schieda N, Hodgdon T, McInnes MD, Dilauro M, Flood TA. Angiomyolipoma (AML) without visible fat: Ultrasound, CT and MR imaging features with pathological correlation. Eur Radiol 2016;26:592–600. [PubMed: 26032880]
12. Gurr MI, Harwood J, Frayn KN. Lipid biochemistry: An introduction. New York: John Wiley & Sons; 2002.
13. Del Grande F, Santini F, Herzka DA, et al. Fat-suppression techniques for 3-T MR imaging of the musculoskeletal system. Radiographics 2014; 34:217–233. [PubMed: 24428292]
14. Zhang J, Pedrosa I, Rofsky NM. MR techniques for renal imaging. Radiol Clin N Am 2003;41:877–907. [PubMed: 14521200]
15. Merkle EM, Nelson RC. Dual gradient-echo in-phase and opposed-phase hepatic MR imaging: A useful tool for evaluating more than fatty infiltration or fatty sparing. Radiographics 2006;26:1409–1418. [PubMed: 16973772]
16. Adam SZ, Nikolaidis P, Horowitz JM, et al. Chemical shift MR imaging of the adrenal gland: Principles, pitfalls, and applications. Radiographics 2016;36:414–432. [PubMed: 26849154]
17. Israel GM, Hindman N, Hecht E, Krinsky G. The use of opposed-phase chemical shift MRI in the diagnosis of renal angiomyolipomas. AJR Am J Roentgenol 2005;184:1868–1872. [PubMed: 15908544]
18. Schieda N, Avruch L, Flood TA. Small (<1 cm) incidental echogenic renal cortical nodules: Chemical shift MRI outperforms CT for confirmatory diagnosis of angiomyolipoma (AML). Insights Imaging 2014;5:295–299. [PubMed: 24609721]
19. Rosenkrantz AB, Raj S, Babb JS, Chandarana H. Comparison of 3D two-point Dixon and standard 2D dual-echo breath-hold sequences for detection and quantification of fat content in renal angiomyolipoma. Eur J Radiol 2012;81:47–51. [PubMed: 21126839]
20. Outwater EK, Bhatia M, Siegelman ES, Burke MA, Mitchell DG. Lipid in renal clear cell carcinoma: Detection on opposed-phase gradient-echo MR images. Radiology 1997;205:103–107. [PubMed: 9314970]
21. Outwater EK, Mitchell DG. Differentiation of adrenal masses with chemical shift MR imaging. Radiology 1994;193:877–878. [PubMed: 7972841]
22. Outwater EK, Siegelman ES, Radecki PD, Piccoli CW, Mitchell DG. Distinction between benign and malignant adrenal masses: Value of T1-weighted chemical-shift MR imaging. AJR Am J Roentgenol 1995; 165:579–583. [PubMed: 7645474]
23. Schieda N, Kiezlar AZ, Al Dandan O, McInnes MD, Flood TA. Ten uncommon and unusual variants of renal angiomyolipoma (AML): Radiologic-pathologic correlation. Clin Radiol 2015;70:206–220. [PubMed: 25468637]
24. Helenon O, Merran S, Paraf F, et al. Unusual fat-containing tumors of the kidney: A diagnostic dilemma. Radiographics 1997;17:129–144. [PubMed: 9017804]
25. D'Angelo PC, Gash JR, Horn AW, Klein FA. Fat in renal cell carcinoma that lacks associated calcifications. AJR Am J Roentgenol 2002;178: 931–932. [PubMed: 11906875]
26. Schuster TG, Ferguson MR, Baker DE, Schaldenbrand JD, Solomon MH. Papillary renal cell carcinoma containing fat without calcification mimicking angiomyolipoma on CT. AJR Am J Roentgenol 2004;183:1402–1404. [PubMed: 15505311]

27. Richmond L, Atri M, Sherman C, Sharir S. Renal cell carcinoma containing macroscopic fat on CT mimics an angiomyolipoma due to bone metaplasia without macroscopic calcification. Br J Radiol 2010;83:e179–181. [PubMed: 20647509]
28. Heye S, Woestenborghs H, Van Kerkhove F, Oyen R. Adrenocortical carcinoma with fat inclusion: Case report. Abdom Imaging 2005;30: 641–643. [PubMed: 15688105]
29. Egbert N, Elsayes KM, Azar S, Caoili EM. Computed tomography of adrenocortical carcinoma containing macroscopic fat. Cancer Imaging 2010;10:198–200.
30. Kenney PJ, Wagner BJ, Rao P, Heffess CS. Myelolipoma: CT and pathologic features. Radiology 1998;208:87–95. [PubMed: 9646797]
31. Shaaban AM, Rezvani M, Tubay M, Elsayes KM, Woodward PJ, Menias CO. Fat-containing retroperitoneal lesions: Imaging characteristics, localization, and differential diagnosis. Radiographics 2016;36: 710–734. [PubMed: 27163589]
32. Blake MA, Kalra MK, Maher MM, et al. Pheochromocytoma: An imaging chameleon. Radiographics 2004;24(Suppl 1):S87–99. [PubMed: 15486252]
33. Newhouse JH, Heffess CS, Wagner BJ, Imray TJ, Adair CF, Davidson AJ. Large degenerated adrenal adenomas: Radiologic-pathologic correlation. Radiology 1999;210:385–391. [PubMed: 10207419]
34. Montone KT, Rosen M, Siegelman ES, Fogt F, Livolsi VA. Adrenocortical neoplasms with myelolipomatous and lipomatous metaplasia: Report of 3 cases. Endocr Pract 2009;15:128–133. [PubMed: 19289323]
35. Eble JN SG, Epstein JI, Sesterhenn IA. World Health Organization classification of tumors: Pathology and genetics of tumors of the urinary system and male genital organs World Health Organization Classification of Tumors. Vol. 2013 Lyon, France; 2004.
36. Chen CL, Tang SH, Wu ST, et al. Calcified, minimally fat-contained angiomyolipoma clinically indistinguishable from a renal cell carcinoma. BMC Nephrol 2013;14:160. [PubMed: 23876081]
37. Cholet C, Eiss D, Cohen D, Verkarre V, Helenon O. Calcified renal angiomyolipoma: A case report. Urology 2016;97:e7–e8. [PubMed: 27443470]
38. Deeths TM, Melson GL. Calcification in an angiomyolipoma: A case report. J Urol 1975;114:613–614. [PubMed: 1235391]
39. Ferrozzi F, Bova D. CT and MR demonstration of fat within an adrenal cortical carcinoma. Abdom Imaging 1995;20:272–274. [PubMed: 7620426]
40. Rofsky NM, Bosniak MA, Megibow AJ, Schlossberg P. Adrenal myelolipomas: CT appearance with tiny amounts of fat and punctate calcification. Urol Radiol 1989;11:148–152. [PubMed: 2595871]
41. Cornelis F, Tricaud E, Lasserre AS, et al. Routinely performed multiparametric magnetic resonance imaging helps to differentiate common sub-types of renal tumours. Eur Radiol 2014;24:1068–1080. [PubMed: 24557052]
42. Cornelis F, Grenier N. Multiparametric magnetic resonance imaging of solid renal tumors: A practical algorithm. Semin Ultrasound CT MR 2017; 38:47–58. [PubMed: 28237280]
43. Hindman N, Ngo L, Genega EM, et al. Angiomyolipoma with minimal fat: Can it be differentiated from clear cell renal cell carcinoma by using standard MR techniques? Radiology 2012;265:468–477. [PubMed: 23012463]
44. Canvasser NE, Kay FU, Xi Y, et al. Diagnostic accuracy of multiparametric magnetic resonance imaging to identify clear cell renal cell carcinoma in cT1a renal masses. J Urol 2017;198:780–786. [PubMed: 28457802]
45. Sasiwimonphan K, Takahashi N, Leibovich BC, Carter RE, Atwell TD, Kawashima A. Small (<4 cm) renal mass: Differentiation of angiomyolipoma without visible fat from renal cell carcinoma utilizing MR imaging. Radiology 2012;263:160–168. [PubMed: 22344404]
46. Schieda N, Dilauro M, Moosavi B, et al. MRI evaluation of small (<4cm) solid renal masses: Multivariate modeling improves diagnostic accuracy for angiomyolipoma without visible fat compared with univariate analysis. Eur Radiol 2016;26:2242–2251. [PubMed: 26486936]
47. Murray CA, Quon M, McInnes MD, et al. Evaluation of T1-weighted MRI to detect intratumoral hemorrhage within papillary renal cell carcinoma as a feature differentiating from

angiomyolipoma without visible fat. AJR Am J Roentgenol 2016;207:585–591. [PubMed: 27275530]

48. Schieda N, Hodgdon T, El-Khodary M, Flood TA, McInnes MD. Unenhanced CT for the diagnosis of minimal-fat renal angiomyolipoma. AJR Am J Roentgenol 2014;203:1236–1241. [PubMed: 25415700]
49. Hodgdon T MM, Schieda N, Lamb L, Flood TA, Thornhill R. Quantitative CT texture analysis: Can it differentiate between minimal fat renal angiomyolipoma (mfAML) and renal cell carcinoma on non-contrast enhanced computed tomography (NECT)? Radiology 2015;276:787–796. [PubMed: 25906183]
50. Sun MR, Ngo L, Genega EM, et al. Renal cell carcinoma: Dynamic contrast-enhanced MR imaging for differentiation of tumor subtypes— Correlation with pathologic findings. Radiology 2009;250:793–802. [PubMed: 19244046]
51. Herts BR, Coll DM, Novick AC, et al. Enhancement characteristics of papillary renal neoplasms revealed on triphasic helical CT of the kidneys. AJR Am J Roentgenol 2002;178:367–372. [PubMed: 11804895]
52. Kim JK, Kim SH, Jang YJ, et al. Renal angiomyolipoma with minimal fat: Differentiation from other neoplasms at double-echo chemical shift FLASH MR imaging. Radiology 2006;239:174–180. [PubMed: 16507752]
53. Jhaveri KS, Elmi A, Hosseini-Nik H, et al. Predictive value of chemical-shift MRI in distinguishing clear cell renal cell carcinoma from non-clear cell renal cell carcinoma and minimal-fat angiomyolipoma. AJR Am J Roentgenol 2015;205:W79–86. [PubMed: 26102422]
54. Ferre R, Cornelis F, Verkarre V, et al. Double-echo gradient chemical shift MR imaging fails to differentiate minimal fat renal angiomyolipomas from other homogeneous solid renal tumors. Eur J Radiol 2015;84:360–365. [PubMed: 25547327]
55. Chen LS, Zhu ZQ, Wang ZT, et al. Chemical shift magnetic resonance imaging for distinguishing minimal-fat renal angiomyolipoma from renal cell carcinoma: A meta-analysis. Eur Radiol 2018;28:1854–1861. [PubMed: 29178029]
56. Gabriel H, Pizzitola V, McComb EN, Wiley E, Miller FH. Adrenal lesions with heterogeneous suppression on chemical shift imaging: Clinical implications. J Magn Reson Imaging 2004;19:308–316. [PubMed: 14994299]
57. Schwartz LH, Macari M, Huvos AG, Panicek DM. Collision tumors of the adrenal gland: Demonstration and characterization at MR imaging. Radiology 1996;201:757–760. [PubMed: 8939227]
58. Haider MA, Ghai S, Jhaveri K, Lockwood G. Chemical shift MR imaging of hyperattenuating (>10 HU) adrenal masses: Does it still have a role? Radiology 2004;231:711–716. [PubMed: 15118113]
59. Weiss LM, Medeiros LJ, Vickery AL Jr. Pathologic features of prognostic significance in adrenocortical carcinoma. Am J Surg Pathol 1989;13: 202–206. [PubMed: 2919718]
60. Blake MA, Krishnamoorthy SK, Boland GW, et al. Low-density pheochromocytoma on CT: A mimicker of adrenal adenoma. AJR Am J Roentgenol 2003;181:1663–1668. [PubMed: 14627592]
61. Schieda N, Alrashed A, Flood TA, Samji K, Shabana W, McInnes MD. Comparison of quantitative MRI and CT washout analysis for differentiation of adrenal pheochromocytoma from adrenal adenoma. AJR Am J Roentgenol 2016;206:1141–1148. [PubMed: 27011100]
62. Borhani AA, Hosseinzadeh K. Quantitative versus qualitative methods in evaluation of T2 signal intensity to improve accuracy in diagnosis of pheochromocytoma. AJR Am J Roentgenol 2015;205:302–310. [PubMed: 26204279]
63. Choi YA, Kim CK, Park BK, Kim B. Evaluation of adrenal metastases from renal cell carcinoma and hepatocellular carcinoma: Use of delayed contrast-enhanced CT. Radiology 2013;266:514–520. [PubMed: 23151828]
64. Schieda N, Krishna S, McInnes MD, et al. Utility of MRI to differentiate clear cell renal cell carcinoma adrenal metastases from adrenal adenomas. AJR Am J Roentgenol 2017;209:W152–W159. [PubMed: 28742373]
65. Sasaguri K, Takahashi N, Takeuchi M, Carter RE, Leibovich BC, Kawashima A. Differentiation of benign from metastatic adrenal masses in patients with renal cell carcinoma on contrast-enhanced CT. AJR Am J Roentgenol 2016;207:1031–1038. [PubMed: 27556736]

66. Qiu B, Ackerman D, Sanchez DJ, et al. HIF2alpha-dependent lipid storage promotes endoplasmic reticulum homeostasis in clear-cell renal cell carcinoma. Cancer Discov 2015;5:652–667. [PubMed: 25829424]

67. Kay FU, Canvasser NE, Xi Y, et al. Diagnostic performance and interreader agreement of a standardized MR imaging approach in the prediction of small renal mass histology. Radiology 2018;287:543–553. [PubMed: 29390196]

68. Karlo CA, Donati OF, Burger IA, et al. MR imaging of renal cortical tumours: Qualitative and quantitative chemical shift imaging parameters. Eur Radiol 2013;23:1738–1744. [PubMed: 23300041]

69. Schieda N, van der Pol CB, Moosavi B, McInnes MD, Mai KT, Flood TA. Intracellular lipid in papillary renal cell carcinoma (RCC) at chemical-shift MRI: Radiologic-pathologic correlation. Eur Radiol 2015;25:2134–2142. [PubMed: 25678078]

70. Dixon WT. Simple proton spectroscopic imaging. Radiology 1984;153: 189–194. [PubMed: 6089263]

71. Reeder SB, Sirlin CB. Quantification of liver fat with magnetic resonance imaging. Magn Reson Imaging Clin N Am 2010;18:337–357, ix. [PubMed: 21094444]

72. Reeder SB, McKenzie CA, Pineda AR, et al. Water-fat separation with IDEAL gradient-echo imaging. J Magn Reson Imaging 2007;25:644–652. [PubMed: 17326087]

73. Reeder SB, Wen Z, Yu H, et al. Multicoil Dixon chemical species separation with an iterative least-squares estimation method. Magn Reson Med 2004;51:35–45. [PubMed: 14705043]

74. Yu H, Shimakawa A, McKenzie CA, Brodsky E, Brittain JH, Reeder SB. Multiecho water-fat separation and simultaneous R2* estimation with multifrequency fat spectrum modeling. Magn Reson Med 2008;60: 1122–1134. [PubMed: 18956464]

75. Costa DN, Pedrosa I, McKenzie C, Reeder SB, Rofsky NM. Body MRI using IDEAL. AJR Am J Roentgenol 2008;190:1076–1084. [PubMed: 18356458]

76. Zhang Y, Udayakumar D, Cai L, et al. Addressing metabolic heterogeneity in clear cell renal cell carcinoma with quantitative Dixon MRI. JCI Insight 2017;2:15.

77. van Zijl PC, Jones CK, Ren J, Malloy CR, Sherry AD. MRI detection of glycogen in vivo by using chemical exchange saturation transfer imaging (glycoCEST). Proc Natl Acad Sci U S A 2007;104:4359–4364. [PubMed: 17360529]

CME Information: Renal and adrenal masses containing fat at MRI: Proposed Nomenclature by the Society of Abdominal Radiology Disease-Focused Panel on Renal Cell Carcinoma.

If you wish to receive credit for this activity, please refer to the website: www.wileyhealthlearning.com/reprints

Educational Objectives

Upon completion of this educational activity, participants will be better able to apply terms describing the presence of fat in renal and adrenal masses and communicate imaging findings pertaining to the presence of fat in renal and adrenal masses and the implication of these findings for diagnosis.

Activity Disclosures

No commercial support has been accepted related to the development or publication of this activity.

Faculty Disclosures:

Editor–in–Chief: Mark E. Schweitzer, MD, discloses consultant fees from MCRA and MMI.

CME Editor: Mustafa R. Bashir, MD, discloses research support from GE Healthcare, Madrigal Pharmaceuticals, NGM Biopharmaceuticals, Siemens Healthcare and Taiwan J Pharma, and consultant fees from RadMD.

CME Committee: Bonnie Joe, MD, PhD, discloses author royalties from UpToDate.

Tim Leiner, MD, PhD, discloses research grants from Bayer Healthcare and Philips Healthcare.

Shreyas Vasanawala, MD, PhD, discloses research support from GE Healthcare, and founder's equity in Arterys.

Eric Chang, MD, Feng Feng, MD, and Bruno Madore, PhD; no conflicts of interest or financial relationships relevant to this article were reported.

Authors:

Authors Nicola Schieda MD, Matthew S Davenport MD PhD, Ivan Pedrosa MD, Atul Shinagare MD, Hersch Chandarana MD PhD, Nicole Curci MD, Ankur Doshi MD, Gary Israel, MD, Erick Remer, MD, Jane Wang, MD and Stuart G Silverman MD reported no conflicts of interest or financial relationships relevant to this article. This activity underwent peer review in line with the standards of editorial integrity and publication ethics. Conflicts of interest have been identified and resolved in accordance with John Wiley and Sons, Inc.'s Policy on Activity Disclosure and Conflict of Interest.

Accreditation

John Wiley and Sons, Inc. is accredited by the Accreditation Council for Continuing Medical Education to provide continuing medical education for physicians.

John Wiley and Sons, Inc. designates this journal-based CME activity for a maximum of 1.0 *AMA PRA Category 1 Credit™*. Physicians should only claim credit commensu-rate with the extent of their participation in the activity.

For information on applicability and acceptance of continuing medical education credit for this activity, please consult your professional licensing board.

This activity is designed to be completed within 1 hour. To successfully earn credit, participants must complete the activity during the valid credit period, which is up to two years from initial publication. Additionally, up to 3 attempts and a score of 70% or better is needed to pass the post test.

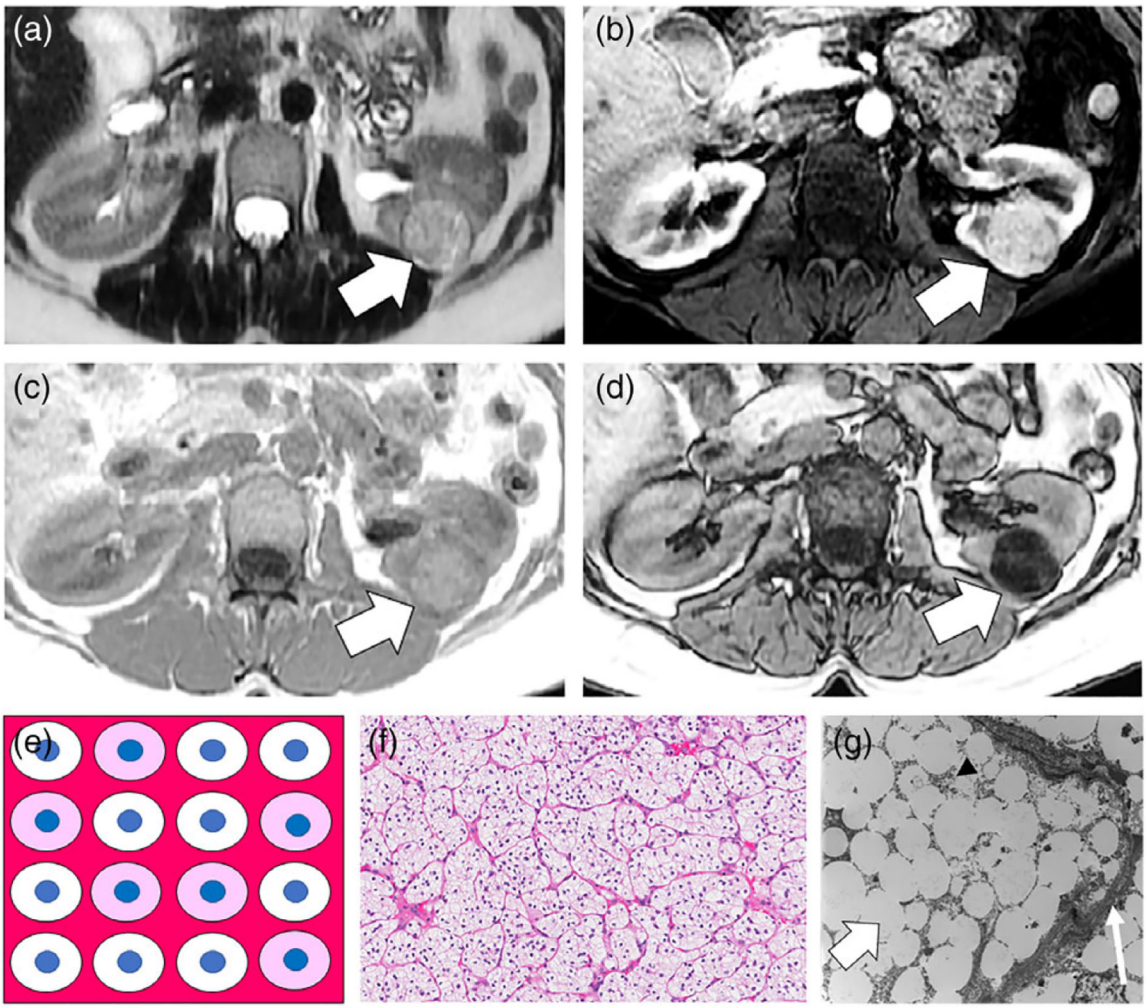

FIGURE 1:

A 53-year-old female with Fuhrman nuclear grade 2 clear cell renal cell carcinoma (RCC) of the left kidney. A: Axial T_2-weighted (T_2W) single-shot fast spin echo (FSE) image shows the tumor is heterogeneously hyperintense (white arrow) compared with the renal cortex. B: Axial T_1-weighted (T_1W) fat-suppressed (FS) gradient recalled echo (GRE) image obtained during the corticomedullary (CM) phase of enhancement shows the tumor (white arrow) is avidly enhancing. C,D: Axial T_1W in-phase (IP) and opposed-phase (OP) dual-echo GRE images shows diffuse nonlinear noncurvilinear loss of signal intensity within the tumor on OP compared with IP images, indicating the presence of microscopic fat. In this patient, the finding was misinterpreted as representing macroscopic fat and the mass was diagnosed as an angiomyolipoma (AML). The correct diagnosis of clear-cell RCC was provided on a second-opinion MRI request and partial nephrectomy was performed. E: Schematic for explanation of signal intensity loss on OP MRI in clear-cell RCC. The tumor consists of cells that contain a variable amount of intracytoplasmic fat and glycogen, which when processed will appear optically clear (in this schematic white). Other cells that do not contain intracytoplasmic lipid and glycogen show typical light pink cytoplasm. The blue dots represent the nucleus in the background of stroma and a capillary network characteristic

of clear-cell RCC. A variable amount of stroma including a rich thin arborizing vasculature (at pathology often referred to as “chicken wire”) is characteristic in clear-cell RCC (dark pink). There are no adipocytes (fat cells) within the tumor. F: High-power (20×) microscopic image of the tumor stained with hematoxylin and eosin (H&E) show the abundance of cells with clear cytoplasm surrounded by a network of capillaries. G: Transmission electron microscope image (5000×) shows the abundance of fat droplets (thick white arrow) within the cell which is surrounded by the cell membrane (thin white arrow). Stippled black dots (arrowhead) represent glycogen molecules within the cytoplasm.

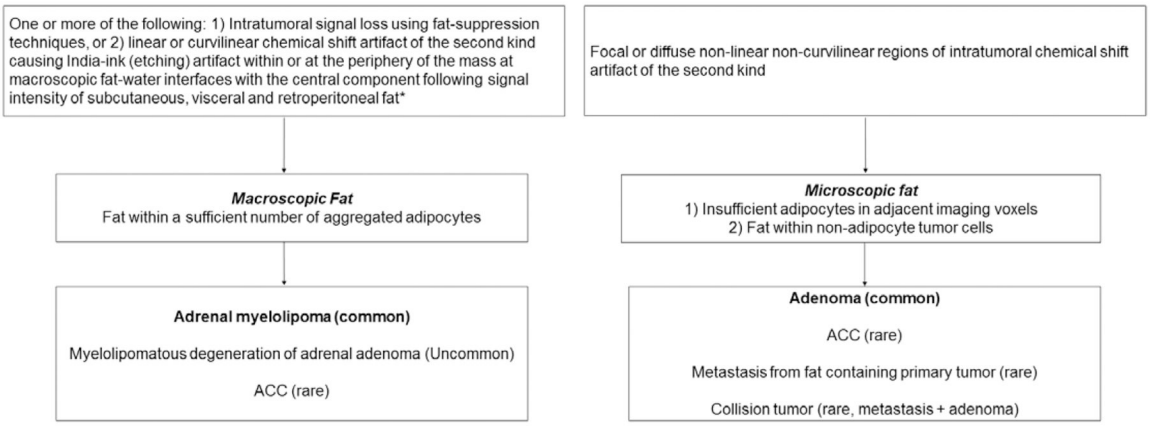

FIGURE 2:

Flow diagram for proposed nomenclature to improve description of intratumoral fat in adrenal masses at MRI. ACC = adrenal cortical carcinoma. *When CSI is performed using a 2- or 3-point Dixon technique, a third feature that is diagnostic of macroscopic fat is the presence of increased signal intensity (isointense to the subcutaneous, visceral, and retroperitoneal fat) on fat-only data sets.

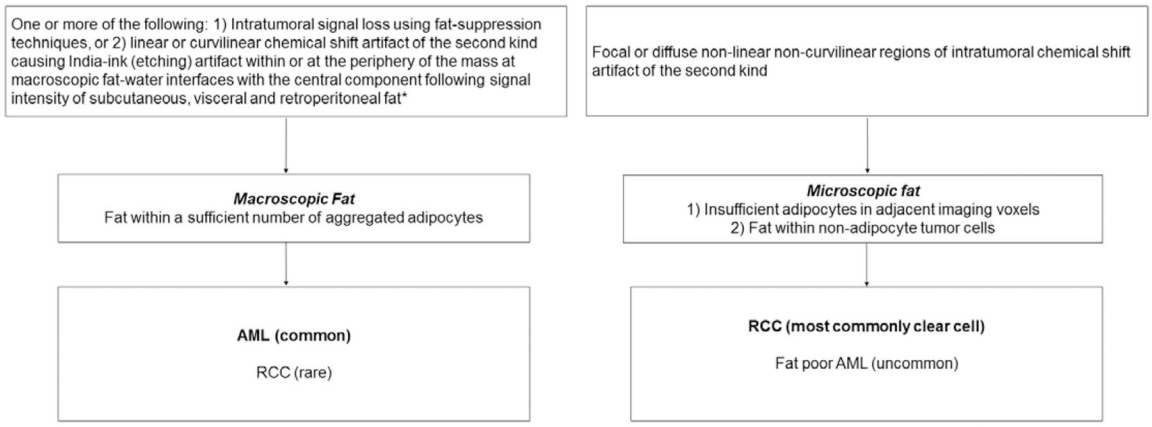

FIGURE 3:

Flow diagram for proposed nomenclature to improve description of intratumoral fat in renal masses at MRI. AML = angiomyolipoma. *When CSI is performed using a 2- or 3-point Dixon technique, a third feature that is diagnostic of macroscopic fat is the presence of increased signal intensity (isointense to the subcutaneous, visceral and retroperitoneal fat) on fat-only datasets.

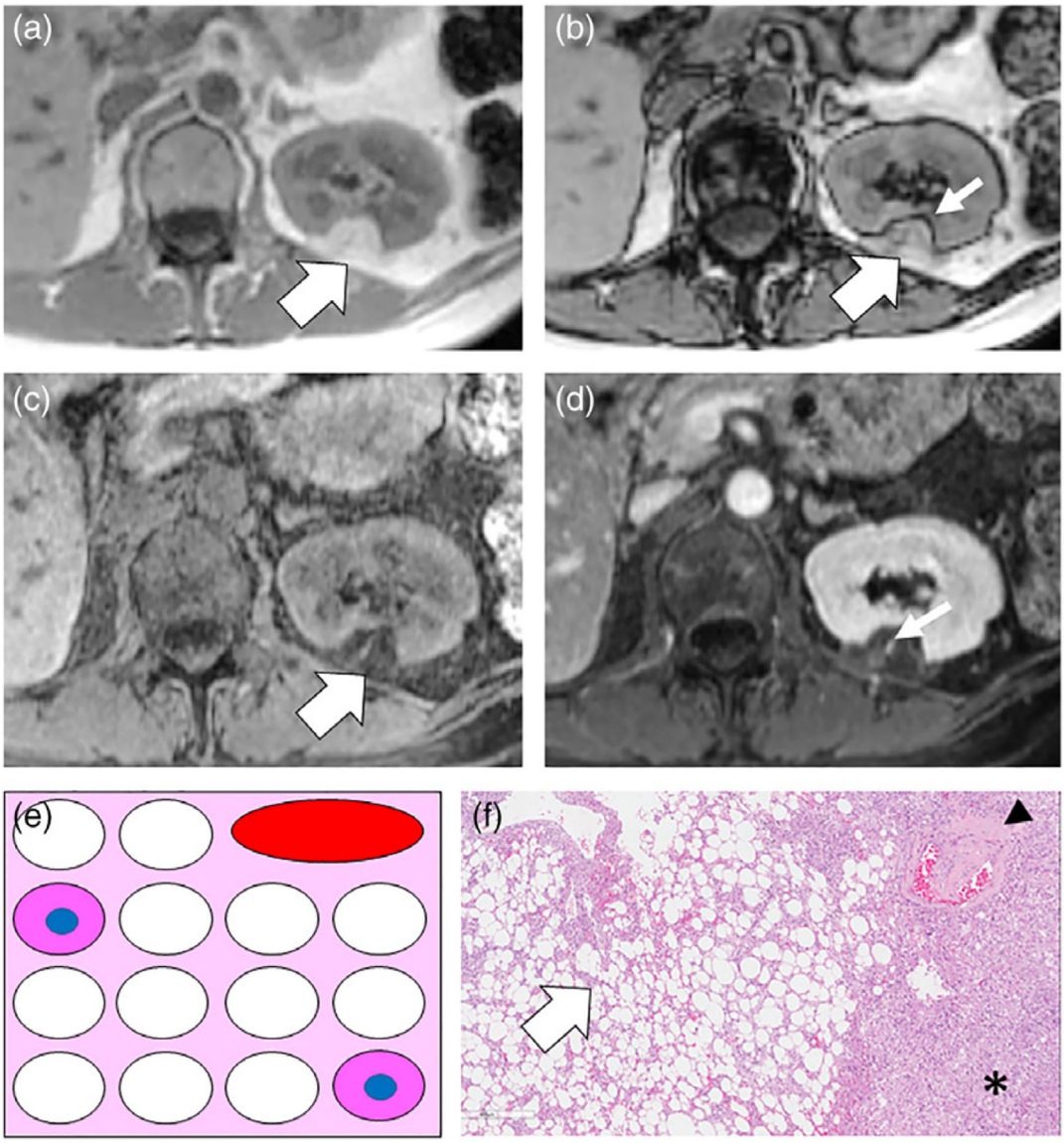

FIGURE 4:

A 42-year-old female with classic left interpolar AML. A,B: Axial T_1W IP and OP dual-echo GRE images show a T_1W hyperintense mass in the posterior interpolar region of the left kidney (white arrows) isointense to retroperitoneal fat. Note linear India-ink (etching) chemical shift artifact of the second kind (thin white arrow) where the mass interfaces with the kidney (macroscopic fat water interface) indicating that the mass is composed of macroscopic fat. C: Axial T_1W chemical FS GRE image shows homogeneous suppression of signal (white arrow) that is another method to confirm macroscopic fat content. D: Axial T_1W FS gadolinium enhanced GRE image obtained during the nephrographic (NG) phase shows enhancement of a vessel within the AML. E: Schematic for explanation of macroscopic fat in classic AML. The tumor is composed of varying amounts of smooth muscle cells (pink cytoplasm) and large blood vessels (red oval) and in this case has a large number of aggregated adipocytes (fat cells represented as white cells without nuclei) in the

background of intervening stroma. F: Low-power (5×) H&E-stained microscopic image of AML shows a large number of aggregated adipocytes (white arrow), an immature blood vessel (arrowhead), and smooth muscle (asterisk).

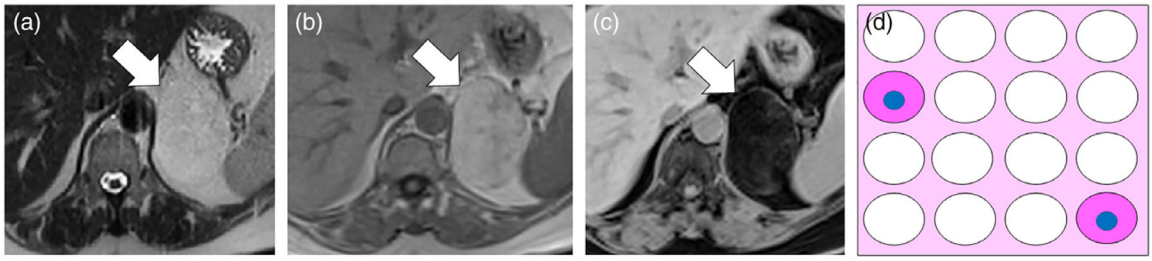

FIGURE 5:

A 61-year-old man with left adrenal myelolipoma. A: Axial single-shot T_2W FSE image shows a homogeneously hyperintense mass in the left adrenal gland (white arrow) that is isointense to retroperitoneal fat. B: Axial T_1W IP GRE image shows the mass (white arrow) is homogeneously hyperintense and isointense to retroperitoneal fat. C: Axial FS T_1W GRE image shows homogeneous suppression of signal within the mass, confirming the presence of macroscopic fat. The mass is composed of greater than 50% macroscopic fat and a diagnosis of myelolipoma was established. The mass remained stable on imaging follow-up for 5 years (not shown). D: Schematic for explanation of macroscopic fat in myelolipoma, analogous to the schematic representation for renal AML (Fig. 4). The tumor is composed of varying amounts of smooth muscle cells (pink cells with nuclei) and a large number of aggregated adipocytes (white cells without nuclei).

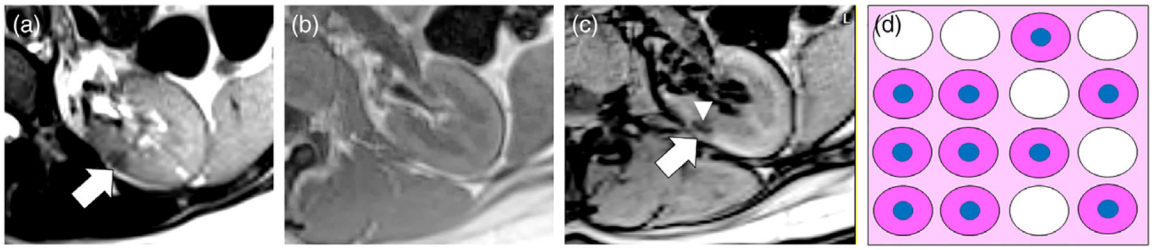

FIGURE 6:

A 44-year-old female with left renal fat-poor angiomyolipoma diagnosed at percutaneous core needle biopsy. A: Axial T_2W FSE image shows a homogeneously hypointense mass in the interpolar region of the left kidney (white arrow). B,C: Axial T_1W IP (B) and OP (C) dual-echo GRE images show nonlinear and noncurvilinear focal area of signal intensity loss within the mass (thin white arrow) on OP MRI due to microscopic fat. The mass was avidly enhancing on corticomedullary phase of gadolinium-enhanced sequences (not shown) D: Schematic for explanation of signal intensity loss on OP images in fat-poor AML. The observation is due to the presence of few or disaggregated adipocytes (white cells without nuclei) with a predominance of smooth muscle cells (pink cells with nuclei).

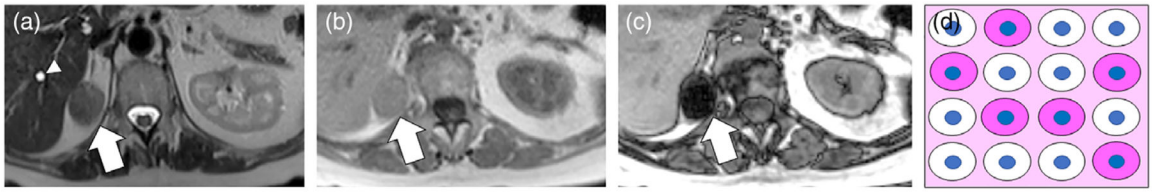

FIGURE 7:

A 42-year-old female with fat-rich (ie, lipid-rich) right adrenal adenoma. A: Axial T_2W FSE image shows a homogeneously hypointense mass in the right adrenal gland (white arrow) and an unrelated simple cyst in segment 7 of the liver (arrowhead). B,C: Axial T_1W IP and OP dual-echo GRE images show homogeneous signal intensity loss within the mass (white arrows) comparing IP and OP MRI due to microscopic fat content. D: Schematic for explanation of signal intensity loss on OP images in adrenal adenomas is similar to schematic for clear cell renal cell carcinomas (Fig. 1). The observation is due to the presence of fat within the cytoplasm of tumor cells rather than the presence of adipocytes.